

Resolving the long-standing enigmas of a giant ornithomimosaur *Deinocheirus mirificus*

Yuong-Nam Lee¹, Rinchen Barsbold², Philip J. Currie³, Yoshitsugu Kobayashi⁴, Hang-Jae Lee¹, Pascal Godefroit⁵, François Escuillié⁶ & Tsogtbaatar Chinzorig²

The holotype of *Deinocheirus mirificus* was collected by the 1965 Polish–Mongolian Palaeontological Expedition at Altan Uul III in the southern Gobi of Mongolia¹. Because the holotype consists mostly of giant forelimbs (2.4 m in length) with scapulocoracoids², for almost 50 years *Deinocheirus* has remained one of the most mysterious dinosaurs. The mosaic of ornithomimosaur and non-ornithomimosaur characters in the holotype has made it difficult to resolve the phylogenetic status of *Deinocheirus*^{3,4}. Here we describe two new specimens of *Deinocheirus* that were discovered in the Nemegt Formation of Altan Uul IV in 2006 and Bugiin Tsav in 2009. The Bugiin Tsav specimen (MPC-D 100/127) includes a left forelimb clearly identifiable as *Deinocheirus* and is 6% longer than the holotype. The Altan Uul IV specimen (MPC-D 100/128) is approximately 74% the size of MPC-D 100/127. Cladistic analysis indicates that *Deinocheirus* is the largest member of the Ornithomimosauria; however, it has many unique skeletal features unknown in other ornithomimosaur, indicating that *Deinocheirus* was a heavily built, non-cursorial animal with an elongate snout, a deep jaw, tall neural spines, a pygostyle, a U-shaped furcula, an expanded pelvis for strong muscle attachments, a relatively short hind limb and broad-tipped pedal unguals. Ecomorphological features in the skull, more than a thousand gastroliths, and stomach contents (fish remains) suggest that *Deinocheirus* was a megaomnivore that lived in mesic environments.

Theropoda Marsh, 1881

Ornithomimosauria Barsbold, 1983

Deinocheiridae Osmólska and Roniewicz, 1970

Deinocheiridae. *Deinocheirus mirificus* and all taxa sharing a more recent common ancestor with it than with *Ornithomimus velox*.

Revised diagnosis of the Deinocheiridae. Ornithomimosaur in which radius and ulna well-separated; flexor tubercle of manual ungual proximally positioned; cnemial crest of tibia projects strongly anterodorsally.

Deinocheirus mirificus Osmólska and Roniewicz, 1970

Holotype. Paleontological Center of Mongolian Academy of Sciences (Ulaanbaatar, Mongolia) MPC-D 100/18 (formerly ZPal MgD-I/6) includes pectoral girdles, forelimbs, and fragments of vertebrae, ribs and gastralia².

Referred material. MPC-D 100/127, nearly complete skeleton lacking mid-dorsal vertebrae, many caudals, and right forelimb. MPC-D 100/128,

post-cervical vertebrae, ilia, partial ischia, and left hind limb (Fig. 1, Supplementary Information and Supplementary Data).

Horizon and localities. Nemegt Formation (Upper Campanian or Lower Maastrichtian) at Altan Uul III (holotype), Altan Uul IV (MPC-D 100/128), and Bugiin Tsav (MPC-D 100/127), Mongolia.

Description. Bivariate comparisons of the skull (1024 mm from premaxilla to occipital condyle) with the femur show that the cranium (Fig. 2) is low and narrow like other ornithomimosaur, but that the antorbital region is more elongate than in other members of this clade. The premaxillae and dentaries expand anterolaterally to form a spatulate beak; the external nares open dorsally. In lateral view, the buccal edges of the premaxilla, maxilla and dentary slope anteroventrally. Pitting of the anterior surfaces indicates the presence of keratinous rhamphotheca in life. The nasal is a narrow strap-like bone extending from the anterior third of the internarial bar to above the orbits. Similar to *Gallimimus*, the jugal and quadratojugal form an extensive posteroventral lobe that closed off the lower part of the infratemporal fenestra⁵. The pneumatic fossa of the quadrate is particularly large, about 30% the height of the bone. The outside diameter of the sclerotic ring (84 mm) is relatively small compared with skull length (Extended Data Fig. 1), which suggests that *Deinocheirus* was probably diurnal⁶. The edentulous lower jaw is strikingly massive and deep in lateral view in comparison with the slender, low edentulous maxilla. It scales with tyrannosaurids in the depth of the jaw, rather than ornithomimids (Extended Data Table 1 and Extended Data Fig. 2).

Each of the ten cervical vertebrae is low and long. Posteriorly the centra become progressively shorter and more trapezoidal in outline; this produces a more strongly S-curved neck (to support the relatively larger skull) than in other ornithomimosaur (Extended Data Fig. 3). Twelve dorsal vertebrae have distinctive configurations; the neural spines of anterior dorsals are low, but increase progressively to that of the last dorsal, which is 8.5 times taller than its centrum height; it almost attains the highest ratio of *Spinosaurus*⁷. Because of the presence of an intricate system of interspinous ligaments, they were probably specialized to support the abdomen from the hips and hind limbs in a manner similar to an asymmetrical cable-stayed bridge. The elongate spines might also have served in display. Dorsal vertebrae have numerous laminae forming basal webbing with associated fossae, and the degree of pneumaticity is comparable with that of a sauropod (Extended Data Fig. 4).

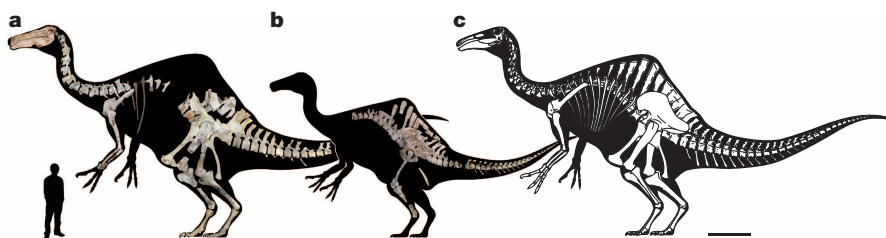


Figure 1 | *Deinocheirus mirificus*. **a**, MPC-D 100/127. **b**, MPC-D 100/128. **c**, Composite reconstruction of MPC-D 100/127 with a simple proportional enlargement of MPC-D 100/128. Scale bar, 1 m. The human outline is 1.7 m tall. The holotype and the two new specimens provide almost all skeletal information of *Deinocheirus*.

¹Geological Museum, Korea Institute of Geoscience and Mineral Resources, Daejeon 305-350, South Korea. ²Paleontological Center, Mongolian Academy of Sciences, Ulaanbaatar 210-351, Mongolia. ³Department of Biological Sciences, University of Alberta, Edmonton, Alberta T6G 2E9, Canada. ⁴Hokkaido University Museum, Hokkaido University, Sapporo 060-0810, Japan. ⁵Earth and History of Life, Royal Belgian Institute of Natural Sciences, Rue Vautier 29, 1000 Bruxelles, Belgium. ⁶Eldonia, 9 Avenue des Portes Occitanes, 3800 Gannat, France.

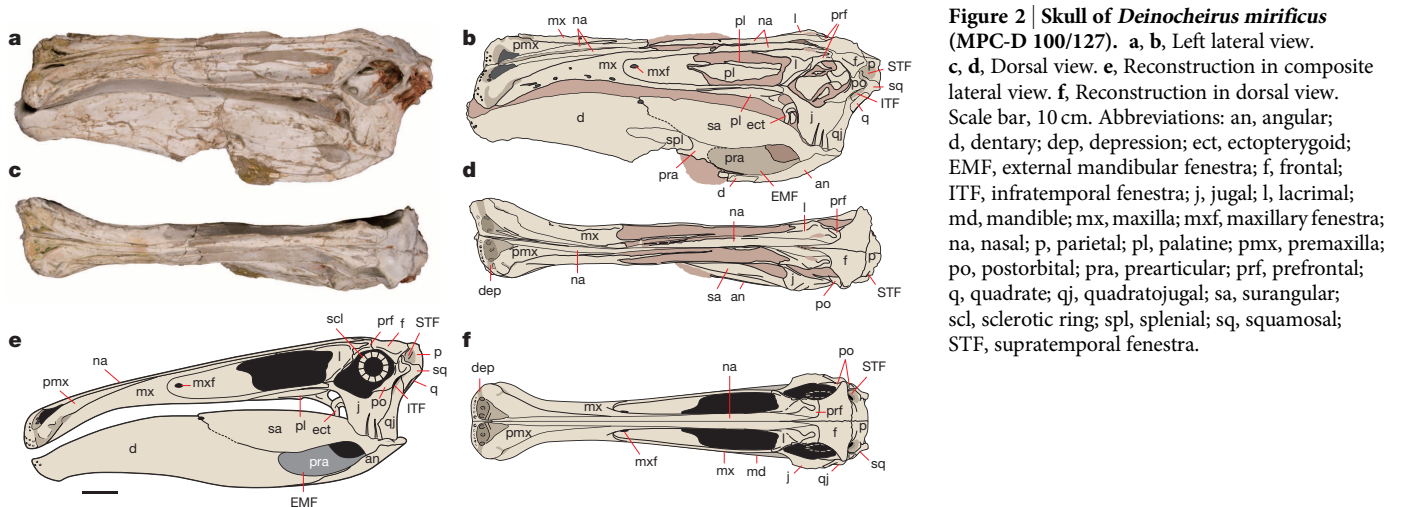


Figure 2 | Skull of *Deinocheirus mirificus* (MPC-D 100/127). **a, b**, Left lateral view. **c, d**, Dorsal view. **e**, Reconstruction in composite lateral view. **f**, Reconstruction in dorsal view. Scale bar, 10 cm. Abbreviations: an, angular; d, dentary; dep, depression; ect, ectopterygoid; EMF, external mandibular fenestra; f, frontal; ITF, infratemporal fenestra; j, jugal; l, lacrimal; md, mandible; mx, maxilla; mxl, maxillary fenestra; na, nasal; p, parietal; pl, palatine; pmx, premaxilla; po, postorbital; pra, prearticular; prf, prefrontal; q, quadrate; qj, quadratojugal; sa, surangular; scl, sclerotic ring; spl, splenial; sq, squamosal; STF, supratemporal fenestra.

All six sacral neural spines are tall and highly pneumatic, extending up to 170% of ilium height. Except for the first sacral, the tops of the sacral neural spines are fused into a midline plate of bone, the dorsal margin of which is straight in lateral view. An accessory spinodiapophyseal lamina is developed anterior to the spinodiapophyseal lamina in each of the third to fifth sacrals. These two laminae meet at the diapophysis to form a unique V-shape in lateral view (Fig. 3).

The first caudal neural spine curves anteriorly in lateral view, and is distinctly shorter than that of the final sacral. The tall anterior caudal neural spines have strong anterior and posterior rugosities with many small foramina for the interarcual ligaments. The end of the tail is

represented by at least two vertebrae that were fused together as in oviraptorosaur and therizinosauroid pygostyles^{8,9}. The presence of a pygostyle suggests the possibility that ornithomimosaurs, which are known to have pennaceous feathers¹⁰, also had fans of feathers at the ends of their tails for display purposes¹¹. Honeycombed camellate pneumatic systems are present in all *Deinocheirus* vertebrae except for the atlas and the distal caudals. Camellate internal structure is also in the parts of the ilium, pubis and ischium that are adjacent to the sacrals. Vertebral pneumaticity correlates with gigantism¹².

A U-shaped furcula with a hypocleidium was recovered for the first time in ornithomimosaurs. The triangular acromial process of the

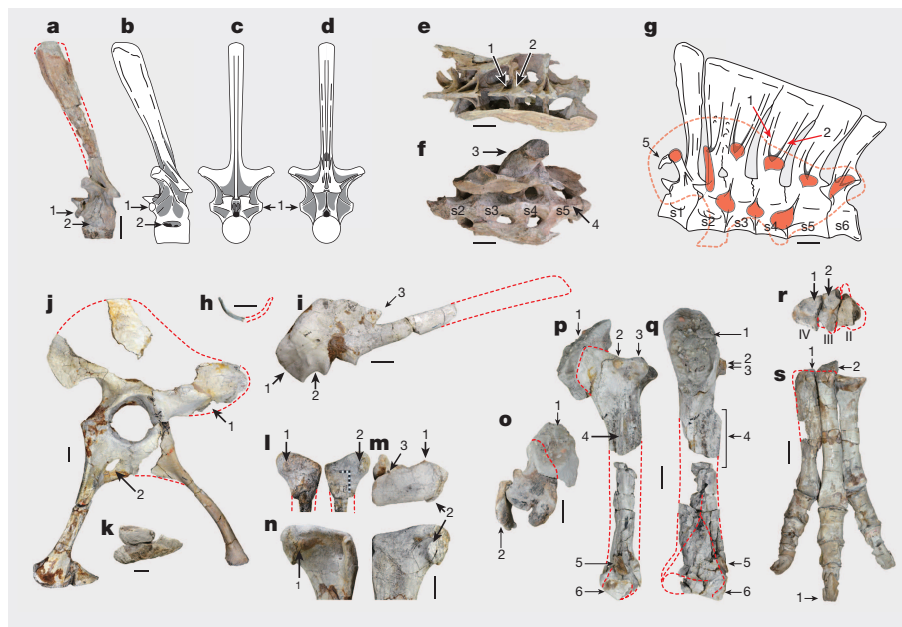


Figure 3 | Postcranial skeletons of *Deinocheirus mirificus* (MPC-D 100/127, MPC-D 100/128). **a–d**, Dorsal vertebra 12 of MPC-D 100/128 (**a**, left lateral view; **b–d**, reconstruction in lateral, anterior, and posterior views; shaded areas indicate fossae; 1, parapophysis; 2, pneumatopore; see Supplementary Information for detailed skeletal anatomy). **e–g**, Sacrum with ilia of MPC-D 100/128 (**e**, dorsal view; **f**, ventral view; **g**, reconstruction of sacrum; orange shading indicates contacts for ilium; 1, accessory spinodiapophyseal lamina; 2, spinodiapophyseal lamina; 3, left proximal femur; 4, sharp ventral keel; 5, diminutive sacral 1 rib). **h**, Furcula of MPC-D 100/127. **i**, Left scapulocoracoid of MPC-D 100/127 (1, subquadrangular coracoid with ventrally extended blade; 2, unexpanded subglenoid fossa; 3, acromial process). **j, k**, Pelvic girdle of MPC-D 100/127 (**j**, lateral view; 1, anteroventrally

inclined brevis fossa; 2, completely enclosed pubic obturator foramen; **k**, pubic boot in distal view). **l–n**, Left femoral heads of MPC-D 100/128 and MPC-D 100/127 (**l**, anterior (left) and posterior (right) views of MPC-D 100/128; **m**, proximal view of MPC-D 100/127; **n**, anterior (left) and posterior (right) views of MPC-D 100/127; 1, dome-like tubercle; 2, pronounced vertical hook; 3, intertrochanteric foramen). **o–q**, Left tibia of MPC-D 100/127 with gastrolith mass *in situ* (**o**, proximal view; **p**, lateral view; **q**, anterior view; 1, gastrolith mass; 2, accessory process; 3, lateral condyle; 4, fibular flange; 5, distal part of fibula; 6, calcaneum). **r, s**, Foot of MPC-D 100/127 (**r**, proximal view of right metatarsal (left–right reversal); 1 and 2, tarsals; **s**, dorsal view of left foot; 1, blunt tip of ungual). All scale bars, 10 cm.

scapulocoracoid prominently projects at an angle of about 50° from the scapular blade. This feature cannot be seen in the holotype due to damage. The ilium appears distinctive because regions of the typical ornithomimosaur pelvis are hypertrophied to support the animal's great weight. The rounded preacetabular ala is taller but anteroposteriorly shorter than the postacetabular ala, which has a concave dorsal margin. The robust supraacetabular crest overhangs the anterodorsal margin of the acetabulum; because the crest was normally directly above the head of the femur, the ilium was tilted posteroventrally in life. The ischium is as long as the pubis.

The femur is longer than the tibia, as expected for such a large animal¹³. In dorsal view, the medial edge of the femoral head has a prominent hook on the posteromedial corner, and a dome-like tubercle on the anterior edge that has never been reported, to our knowledge, in any other dinosaur. The femoral head is twisted 15° anteromedially to the femoral shaft. The robust cnemial crest of the tibia projects above the level of the proximal articular surface as in *Beishanlong*¹⁴ and *Garudimimus*¹⁵. The baseline condition of a relatively short, non-arctometatarsalian metatarsus is present as in most other theropods¹⁶. However, the outline of the proximal end of the third metatarsal in *Deinocheirus* is quadrangular, rather than triangular as in basal ornithomimosaur. The foot is as short in the relative lengths of digit III to metatarsal III as it is in *Garudimimus*. Each pedal ungual has a unique shape that has never been reported, to our knowledge, in any other theropod dinosaur, with the distal end bluntly truncated rather than tapered (Extended Data Fig. 5).

Deinocheirus was coded into a theropod data matrix that incorporated a comprehensive analysis for Ornithomimosauria¹⁷ (Extended Data Fig. 6). It was recovered as a sister taxon of *Garudimimus* within the Ornithomimosauria (Fig. 4). This comprehensive phylogeny suggests that basal ornithomimosaur separated into two lineages (Deinocheiridae and Ornithomimidae) in the Early Cretaceous. The Deinocheiridae consists of *Deinocheirus*, *Garudimimus*, and the older *Beishanlong*. *Deinocheirus* (MPC-D 100/127) had a body length of 11 m and an estimated body weight of 6,358 kg¹⁸, and is the largest known ornithomimosaur. Deinocheirids followed a different evolutionary path from cursorial ornithomimids. Limb proportions suggest that, like *Deinocheirus*, *Garudimimus* was not adapted for speed. Deinocheirids also lack the distinct insertion of the iliofibularis muscle onto the fibular shaft, and in lateral view do not have the straight pedal unguals seen in other ornithomimosaur.

A large number (>1,400) of gastroliths (ranging from 8 to 87 mm) were collected during excavation from inside the ribs and gastralia of MPC-D 100/127. The ratio of gastrolith mass/body mass (approximately 0.0022)¹⁹ suggests that gastroliths were used to grind food in the toothless *Deinocheirus*. Rhamphotheca, edentulous jaws, a U-shaped dentary symphysis, an anteriorly downturned dentary, and a dorsally convex dentary in *Deinocheirus* are known as characters of at least facultative herbivory in Coelurosauria^{20,21}. Interestingly, fish remains (vertebrae and scales) were discovered *in situ* amongst the gastroliths (Extended Data Fig. 7). The stomach contents and various herbivorous ecomorphological features suggest that *Deinocheirus* was omnivorous.

The supratemporal and infratemporal adductor chambers in *Deinocheirus* are strikingly small compared with the elongate, large skull, implying weak bite force. The unique *Deinocheirus* skull morphology and a simple orthal jaw action is more suitable for cropping relatively soft understory vegetation (or possibly herbaceous water plants): skull length correlates negatively with bite force and feeding height (plant height)²². The deep buccal cavity, as evidenced by the deep lower jaws, suggests the presence of a massive tongue that when manipulated would create suction for ingesting the organic material cropped and disturbed by the broad bill as it foraged on the bottom of streams, lakes and ponds. The duck-like bill of *Deinocheirus* may be ecologically tied to water-based food as in ducks²³, as well as ground-level, non-selective browsing as in some genera of sauropods²⁴ and hadrosaurs²⁵.

Stomach contents include fish remains and indicate that *Deinocheirus* frequented freshwater habitats. The short and compact manual claws of *Deinocheirus* are similar morphologically to those of the therizinosaur

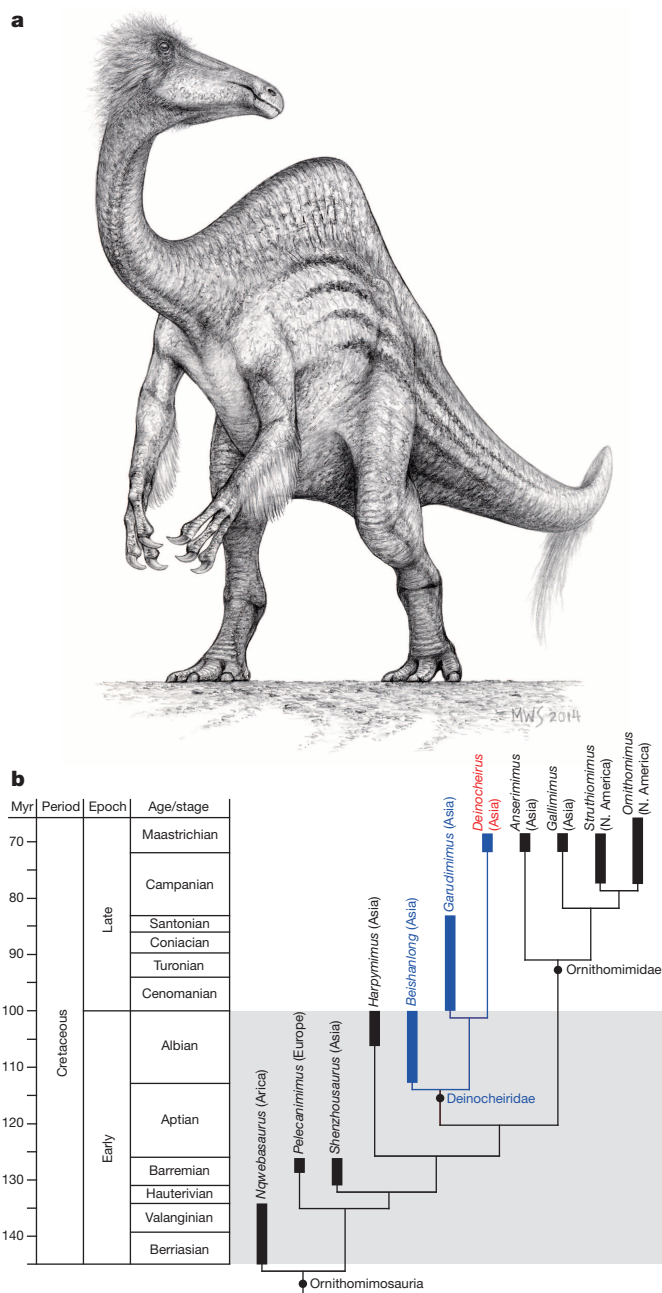


Figure 4 | Phylogenetic relationships of *Deinocheirus mirificus* within Ornithomimosauria. **a**, Hypothetical fleshed-out reconstruction of *Deinocheirus mirificus* (by Michael Skrepnick). **b**, Time-scaled strict consensus tree of the six most-parsimonious trees from our analysis (tree length = 2,927, consistency index = 0.22, retention index = 0.59; Supplementary Information). In this hypothesis *Deinocheirus* is a derived taxon of the Deinocheiridae, which is the sister-group of the Ornithomimidae.

*Alxasaurus*²⁶, which were used in a generalist fashion²⁷. If true, long forearms with giant claws may have been used for digging and gathering herbaceous plants. Robust hind limbs with posteroventrally tilted, wide hips, femora longer than tibiae, and massive feet clearly indicate that *Deinocheirus* was a slow mover. The blunt tips of the pedal unguals would have prevented its feet from sinking deep into wet substrates. The braided or meandering river systems of the Nemegt Formation²⁸ provided a good niche for omnivorous *Deinocheirus* to flourish.

Gigantism may well have been the way *Deinocheirus* escaped predation from *Tarbosaurus* and other theropods of the Nemegt fauna. The trade-off is that it lost the cursorial abilities of its relatives. Ornithomimosauria are normally small to medium-bodied dinosaurs; extending

the allometric trajectories of all known specimens of this clade to gigantic sizes seems to account for many of the peculiar features of *Deinocheirus*, including the elongate forelimbs. The long skull with its broad bill and deep lower jaws demonstrates a more specialized diet than other known ornithomimosaurs. The massive increase in body weight is no doubt responsible for other features, including the increase in neural spine height, and the broad-tipped pedal unguals. Additionally, *Deinocheirus* has at least two features (furculum, pygostyle) previously unknown in ornithomimosaurs, but found in a broad spectrum of other theropods. The discovery of the original specimen almost half a century ago suggested that this was an unusual dinosaur, but did not prepare us for how distinctive *Deinocheirus* is—a true cautionary tale in predicting body forms from partial skeletons, even for animals in which the relationships are known.

Online Content Methods, along with any additional Extended Data display items and Source Data, are available in the online version of the paper; references unique to these sections appear only in the online paper.

Received 9 August; accepted 19 September 2014.

Published online 22 October 2014.

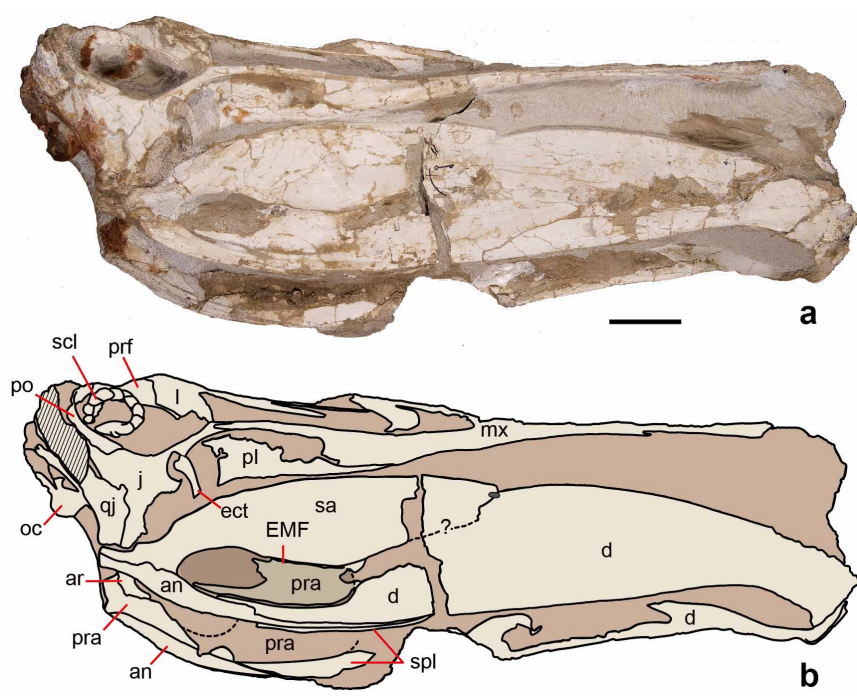
- Kielan-Jaworowska, Z. Third (1965) Polish–Mongolian Palaeontological Expedition to the Gobi Desert and western Mongolia. *Bull. de l'Acad. Pol. Sci. Cl. II* **14**, 249–252 (1966).
- Osmólska, H. & Roniewicz, E. Deinocheiridae, a new family of theropod dinosaurs. *Palaeontol. Polonica* **21**, 5–19 (1970).
- Makovicky, P. J., Kobayashi, Y. & Currie, P. J. in *The Dinosauria* (eds Weishampel, D. B., Dodson, P. & Osmólska, H.) 137–150 (Univ. California Press, 2004).
- Kobayashi, Y. & Barsbold, R. Ornithomimids from the Nemegt Formation of Mongolia. *J. Paleontol. Soc. Korea* **22**, 195–207 (2006).
- Osmólska, H., Roniewicz, E. & Barsbold, R. A new dinosaur *Gallimimus bullatus* n. gen., n. sp. (Ornithomimidae) from the Upper Cretaceous of Mongolia. *Palaeontol. Polonica* **27**, 103–143 (1972).
- Schmitz, L. & Motani, R. Nocturnality in dinosaurs inferred from scleral ring and orbit morphology. *Science* **332**, 705–708 (2011).
- Bailey, J. B. Neural spine elongation in dinosaurs: sailbacks or buffalo-backs? *J. Paleontol.* **71**, 1124–1146 (1997).
- Barsbold, R. *et al.* A pygostyle from a non-avian theropod. *Nature* **403**, 155–156 (2000).
- Xu, X., Cheng, Y., Wang, X. & Chang, C. Pygostyle-like structure from *Beipiaosaurus* (Theropoda, Therizinosaurioidea) from the Lower Cretaceous Yixian Formation of Liaoning, China. *Acta Geol. Sin.* **77**, 294–298 (2003).
- Zelenitsky, D. K. *et al.* Feathered non-avian dinosaurs from North America provide insight into wing origins. *Science* **338**, 510–514 (2012).
- Persons, W. S. IV, Currie, P. J. & Norell, M. A. Oviraptorid tail forms and functions. *Acta Palaeontol. Pol.* **59**, 553–567 (2014).
- Schwarz-Wings, D. *et al.* Mechanical implications of pneumatic neck vertebrae in sauropod dinosaurs. *Proc. R. Soc. B* **277**, 11–17 (2010).
- Currie, P. J. Allometric growth in tyrannosaurids (Dinosauria: Theropoda) from the Upper Cretaceous of North America and Asia. *Can. J. Earth Sci.* **40**, 651–665 (2003).
- Makovicky, P. J. *et al.* A giant ornithomimosaur from the Early Cretaceous of China. *Proc. R. Soc. B* **277**, 191–198 (2010).
- Kobayashi, Y. & Barsbold, R. Reexamination of a primitive ornithomimosaur, *Garudimimus brevipes* Barsbold, 1981 (Dinosauria: Theropoda), from the Late Cretaceous of Mongolia. *Can. J. Earth Sci.* **42**, 1501–1521 (2005).
- Holtz, T. R., Jr. The arctometatarsalian pes, an unusual structure of the metatarsus of Cretaceous Theropoda (Dinosauria: Saurischia). *J. Vertebr. Paleontol.* **14**, 480–519 (1995).
- Choiniere, J. N., Forster, C. A. & de Klerk, W. J. New information on *Nqwebasaurus thwazi*, a coelurosaurian theropod from the Early Cretaceous Kirkwood Formation in South Africa. *J. Afr. Earth Sci.* **71–72**, 1–17 (2012).
- Benson, R. B. J. *et al.* Rates of dinosaur mass body evolution indicate 170 million years of sustained ecological innovation on the avian stem lineage. *PLoS Biol.* **12**, e1001853 (2014).
- Wings, O. & Sander, P. M. No gastric mill in sauropod dinosaurs: new evidence from analysis of gastrolith mass and function in ostriches. *Proc. R. Soc. B* **274**, 635–640 (2007).
- Zanno, L. E. & Makovicky, P. J. Herbivorous ecomorphology and specialization patterns in theropod dinosaur evolution. *Proc. Natl Acad. Sci. USA* **108**, 232–237 (2011).
- Zanno, L. E., Gillette, D. D., Albright, L. B. & Titus, A. L. A new North American therizinosaurid and the role of herbivory in 'predatory' dinosaur evolution. *Proc. R. Soc. B* **276**, 3505–3511 (2009).
- Mallon, J. C. & Anderson, J. S. Skull ecomorphology of magaherbivorous dinosaurs from the Dinosaur Park Formation (Upper Campanian) of Alberta, Canada. *PLoS ONE* **8**, e67182 (2013).
- Norell, M. A., Makovicky, P. J. & Currie, P. J. The beaks of ostrich dinosaurs. *Nature* **412**, 873–874 (2001).
- Whitlock, J. A. Inferences of diplodocid (Sauropoda: Dinosauria) feeding behavior from snout shape and microwear analyses. *PLoS ONE* **6**, e18304 (2011).
- Carrano, M. T., Janis, C. M. & Sepkoski, J. J. Jr. Hadrosaurs as ungulate parallels: lost lifestyles and deficient data. *Acta Palaeontol. Pol.* **44**, 237–261 (1999).
- Russell, D. A. & Dong, Z. The affinities of a new theropod from the Alxa Desert, Inner Mongolia, People's Republic of China. *Can. J. Earth Sci.* **30**, 2107–2127 (1993).
- Lautenschlager, S. Morphological and functional diversity in therizinosaur claws and the implications for theropod claw evolution. *Proc. R. Soc. B* **281**, 20140497 (2014).
- Jerzykiewicz, T. & Russell, D. A. Late Mesozoic stratigraphy and vertebrates of the Gobi Basin. *Cretac. Res.* **12**, 345–377 (1991).

Supplementary Information is available in the online version of the paper.

Acknowledgements Information gained from Zofia Kielan-Jaworowska and Wojtec Skarzynski (who respectively found and excavated the holotype) allowed us to refine the original quarry at Altan Uul III. Thanks go to all members of Korea-Mongolia International Dinosaur Expedition (KID) in 2006 and 2009. The KID expedition was supported by a grant to Y.-N.L. from Hwaseong City, Gyeonggi Province, South Korea. Research support was from Korea Institute of Geosciences and Mineral Resources, Korea and Paleontological Center of Mongolian Academy of Sciences, Mongolia.

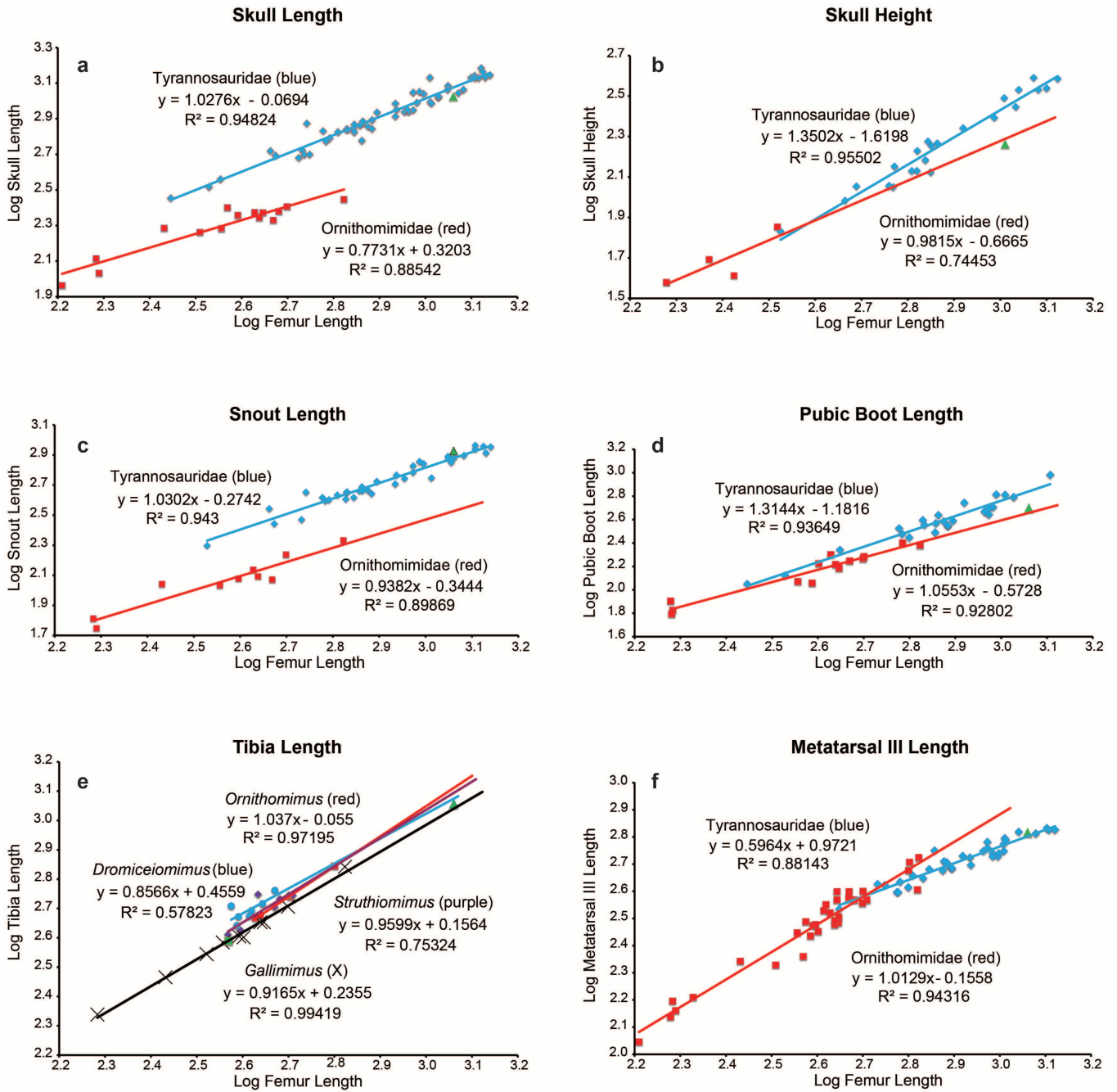
Author Contributions Y.-N.L. designed the project; Y.-N.L., R.B., P.J.C., Y.K. and H.-J.L. collected fossils and performed the research; P.J.C., P.G., F.E. and T.C. helped to repatriate the poached parts of the specimen so that they could be studied. H.-J.L. assembled figures; Y.-N.L. developed and wrote the manuscript with contributions from all authors.

Author Information Reprints and permissions information is available at www.nature.com/reprints. The authors declare no competing financial interests. Readers are welcome to comment on the online version of the paper. Correspondence and requests for materials should be addressed to Y.-N.L. (ylee@kigam.re.kr).



Extended Data Figure 1 | Skull of *Deinocheirus mirificus* (MPC-D 100/127). **a**, In right lateral view. **b**, Line drawing in right lateral view. Scale bar, 10 cm. Abbreviations: an, angular; ar, articular; d, dentary; ect,

ectopterygoid; EMF, external mandibular fenestra; j, jugal; l, lacrimal; mx, maxilla; oc, occipital condyle; pl, palatine; po, postorbital; pra, prearticular; prf, prefrontal; qj, quadratojugal; sa, surangular; scl, sclerotic ring; spl, splenial.

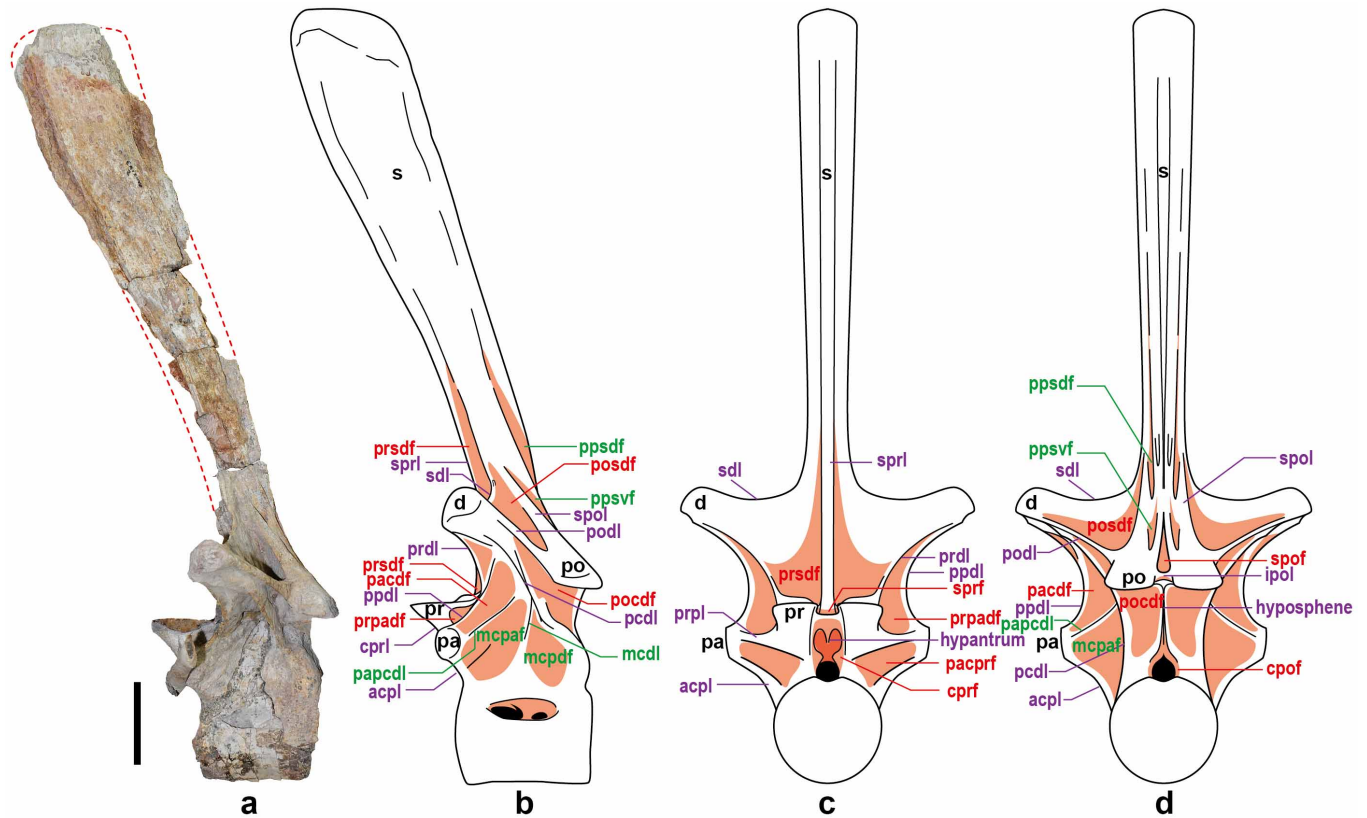


Extended Data Figure 2 | Comparisons of femur length. a, Skull length. b, Skull height. c, Snout length. d, Pubic boot length. e, Tibia length. f, Metatarsal III length in Tyrannosauridae and Ornithomimidae. The green triangle is *Deinocheirus* and the green square is *Garudimimus*.



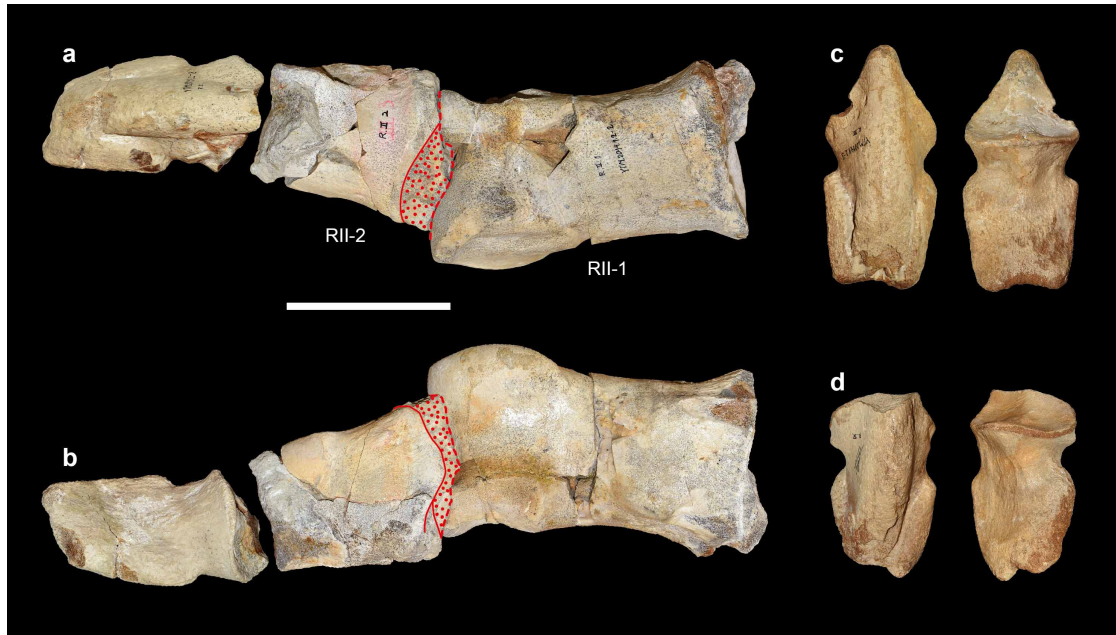
Extended Data Figure 3 | Fourth (upper) and seventh (lower) cervical vertebrae (a–f), and pygostyle (g–l) of *Deinocheirus mirificus* (MPC-D 100/127). a, In anterior view. b, In posterior view. c, In left lateral view. d, In

right lateral view. e, In dorsal view. f, In ventral view. g, In anterior view. h, In posterior view. i, In left lateral view. j, In right lateral view. k, In dorsal view. l, In ventral view. Scale bars, 5 cm.



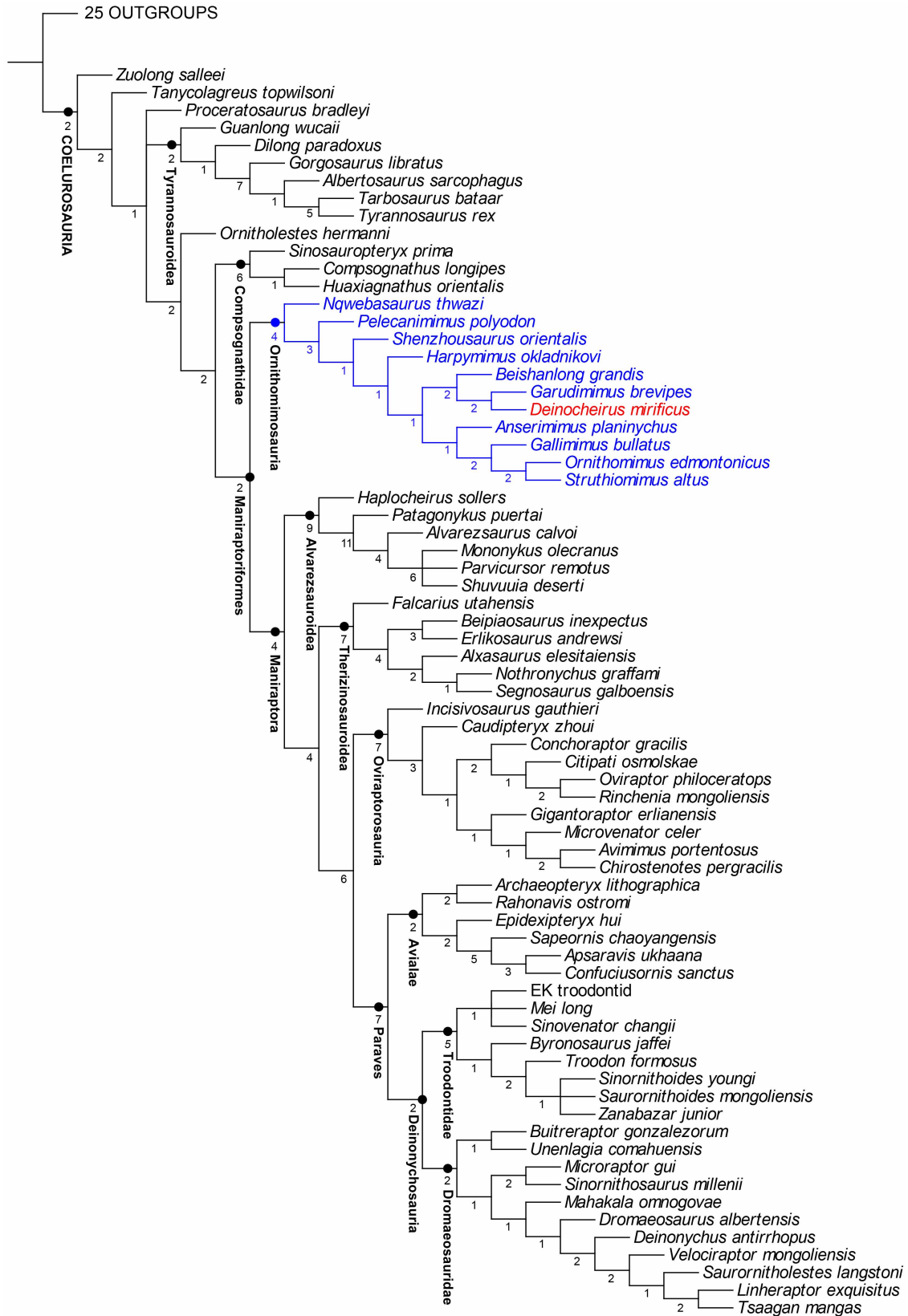
Extended Data Figure 4 | Dorsal vertebra 12 of *Deinocheirus mirificus* (MPC-D 100/128). **a**, Specimen in left lateral view. **b–d**, Reconstructions (**b**, in left lateral view; **c**, in anterior view; **d**, in posterior view). Purple and red colours indicate lamina and fossae, respectively. Green colours indicate new terms used for *Deinocheirus*. Scale bar, 10 cm. Abbreviations: acpl, anterior centroparapophyseal lamina; cporf, centropostzygapophyseal fossa; cprf, centroprezygapophyseal fossa; cprl, centroprezygapophyseal lamina; d, diapophysis; ipol, infrapostzygapophyseal lamina; mccl, middle centriadiapophyseal lamina; mcparf, middle centroparapophyseal fossa; mcpdf, middle centropostdiapophyseal fossa; pa, parapophysis; pacdf, parapophyseal centriadiapophyseal fossa; pacprf, parapophyseal centroprezygapophyseal fossa; papcdl, parapophyseal posterior centriadiapophyseal lamina; pcdl,

posterior centriadiapophyseal lamina; po, postzygapophysis; pocdf, postzygapophyseal centriadiapophyseal fossa; podl, postzygodiapophyseal lamina; posdf, postzygapophyseal spinodiapophyseal fossa; pr, prezygapophysis; ppdl, paradiapophyseal lamina; ppsdf, posterior postzygapophyseal spinodorsal fossa; ppsvf, posterior postzygapophyseal spinovenral fossa; prdl, prezygodiapophyseal lamina; presdf, prezygapophyseal spinodiapophyseal fossa; prpadf, prezygapophyseal paradiapophyseal fossa; prpl, prezygoparapophyseal lamina; prsdf, prezygapophyseal paradiapophyseal fossa; s, neural spine; sdl, spinodiapophyseal lamina; spof, spinopostzygapophyseal fossa; spol, spinopostzygapophyseal lamina; sprf, spinoprezygapophyseal lamina; sprl, spinoprezygapophyseal lamina.

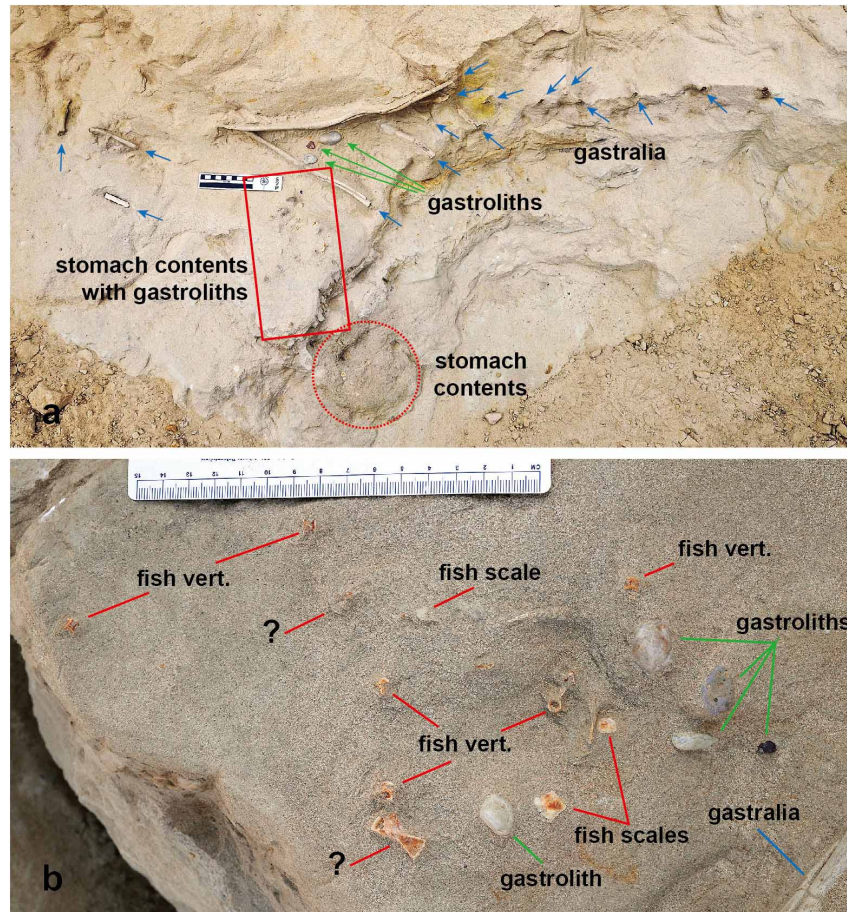


Extended Data Figure 5 | Right pedal digit II and unguals of *Deinocheirus mirificus* (MPC-D 100/127). **a, b,** Digit II in dorsal and ventral views. Isolated right pedal phalanx II-2 was collected in 2009 and perfectly fits into the impression in the matrix attached to the poached phalanx II-1 (the red dot and

solid lines indicate the contact face of the bone boundary with matrix, and the dotted area is matrix). **c,** Ungual of digit III in dorsal and ventral views. **d,** Ungual of digit IV in dorsal and ventral views. Scale bar, 10 cm.



Extended Data Figure 6 | Strict consensus topology of six most parsimonious reconstructions of theropod relationships found in the phylogenetic analysis of 568 characters and 96 taxa. Values indicate Bremer support derived from the BREMER.RUN script supplied by TNT.



Extended Data Figure 7 | Stomach contents of *Deinocheirus mirificus* (MPC-D 100/127). a, Photo to show *in situ* gastralia, gastroliths, and stomach contents. Blue and green arrows represent gastralia and gastroliths.

Red rectangle is an area of scattered fish remains and gastroliths. Red circle is an area where broken fish bones are aggregated. b, Enlarged photo of scattered fish remains (vertebrae, scales) with gastroliths in a.

Extended Data Table 1 | Allometric comparisons between ornithomimosaurids (or ornithomimids) and tyrannosaurids derived from the power equation $y = bx^k$ (solved using logarithmic translation $\log y = k(\log x) + b$)

Taxa	Comparison	n	k	b	R ²
Ornithomimidae	F, Skull	15	0.773	0.32	0.885
Tyrannosauridae	F, Skull	62	1.028	-0.069	0.948
Ornithomimidae	F, Antor	9	0.938	-0.344	0.899
Tyrannosauridae	F, Antor	36	1.03	-0.274	0.943
Ornithomimidae	F, Orb	8	0.509	0.177	0.809
Tyrannosauridae	F, Orb	38	0.47	0.648	0.559
Ornithomimidae	F, Jaw	11	0.787	0.242	0.862
Tyrannosauridae	F, Jaw	43	0.987	0.038	0.96
Tyrannosauridae	F, Jaw H	55	1.391	-1.873	0.887
Ornithomimidae	F, Hum	14	1.165	-0.614	0.956
Tyrannosauridae	F, Hum	40	0.937	-0.339	0.845
Ornithomimidae	F, Rad	18	1.132	-0.667	0.963
Tyrannosauridae	F, Rad	12	0.828	-0.38	0.907
Ornithomimidae	F, Finger II	15	0.815	0.121	0.729
Tyrannosauridae	F, Finger II	22	0.79	-0.094	0.45
Ornithomimidae	F, Ilium	20	1.074	-0.021	0.899
Tyrannosauridae	F, Ilium	50	1.126	-0.351	0.962
Ornithomimidae	F, P Boot	13	1.055	-0.573	0.928
Tyrannosauridae	F, P Boot	21	1.314	-1.182	0.936
Ornithomimidae	F, Ischium	25	1.157	-0.546	0.929
Tyrannosauridae	F, Ischium	32	1.136	-0.529	0.957
Ornithomimidae	F, Fcirc	34	0.986	-0.499	0.986
Tyrannosauridae	F, Fcirc	72	1.336	-1.413	0.935
Ornithomimidae	F, Tibia	55	1.004	0.025	0.983
Tyrannosauridae	F, Tibia	65	0.782	0.621	0.961
Ornithomimidae	F, Mt III	33	1.013	-0.156	0.943
Tyrannosauridae	F, Mt III	36	0.596	0.972	0.881
Ornithomimidae	F, Toe III	13	1.007	-0.337	0.857
Tyrannosauridae	F, Toe III	21	0.825	0.128	0.789

Deinocheirus measurements (Supplementary Data) were compared with the curves of these two lineages to determine whether or not the dimensions of this animal were expected as the result of continued growth trajectories of ornithomimosaurids attaining large size. Growth is isometric when $k = 1$, is negatively allometric when $k < 1$, and positively allometric when $k > 1$. Abbreviations: Antor, Antorbital, snout length; b, constant; Skull, length from premaxilla to occipital condyle; F, femur length; Fcirc, minimum femur shaft circumference; Finger II, second manual digit length; Hum, humerus length; Jaw, mandibular length; Jaw H, mandibular height; k, allometric coefficient; Mt III, metatarsal III; n, sample size; Orb, orbit length; P Boot, pubic boot; R², coefficient of determination; Rad, radius; Toe III, sum of phalangeal lengths of pedal digit III.